Estimating Suspended Particulate Matter Using Remotely Sensed Data: The Case of Mamloo Dam

Mohammad Ranjbar

Abstract— **The Mamloo Dam ecosystem is under constant threat of environmental and anthropogenic stressors owing to its location not far from Jackson, the largest city in Mississippi. While the biological particles in the suspended particulate matter (SPM) including detritus and phytoplankton can be helpful for oyster survival and growth, non-algal suspended silts and clays can negatively affect these suspension feeding animals. This can lead to death by hypoxia/anoxia, to poor health. Oysters are also subjected to additional stress as a result of bio-availability of the contaminants associated with SPM. Runoff from adjacent watersheds and dredging activities increase SPM in the water column. Remote sensing is useful in mapping the spatio-temporal distribution of SPM. The primary objective of this research is to develop remote sensing algorithms for mapping SPM with a focus on non-algal patriciate (NAP) using Moderate Resolution Imaging Spectroradiometer (MODIS) satellite imagery captured in 2015. Water samples and ancillary data were collected from 12 locations within the dam. Semi-analytical algorithms is developed for generating NAP maps using the MODIS satellite imagery and field data. The potential impact of this endeavor will be significant as it informs water managers, the fishery industry, and other stakeholders on the current status of SPM**

Index Terms— **Remote Sensing, Suspended Particulate Matter**

I. INTRODUCTION

Suspended sediments reduces the transmission of solar radiation that shrinks photosynthesis in submerged aquatic vegetation and near-bottom phytoplankton [19]. Diminished photosynthesis means reduction in the size of aquatic vegetation and phytoplankton. The aquatic vegetation and phytoplankton play a vital role in the food chain of the aquatic ecosystem as they are the energy producers in the aquatic environment [19], [20].

Suspended sediments also have direct effect on the health and life of aquatic animals. According to Neil (2006), suspended clay-sized particles rapidly filled the intestinal tract of daphniids eventually leading to starvation.

Suspended sediment also brings toxic substances into lakes, rivers, estuaries, coastal systems, and oceans (Michael et. al 2015). These contaminants affect the population of aquatic animal with short term and long term effects, in which the latter is often not well studied (Michael et. al 2015).

The rate and magnitude of suspended sediments can be affected by factors such as changes in land use, anthropogenic activities, and climate change. The suspended sediments are often transported to coastal bodies by revers joining them.

A. Measuring Suspended Sediments.

Various parameters may be used for describing the concentration and characteristics of suspended sediments according to whether mass or optical properties are of interest and whether particulate matter is sorted into organic/inorganic fractions or not ("total") [2]. The SPM distribution varies in different coastal areas and over a large spatiotemporal domain, hence making the SPM monitoring unprofitable by using traditional field methods, which can provide accurate measurements only at a very small spatiotemporal scale [11].

Remote sensing has become a valuable alternative to in situ measurements [22]. Primarily using data acquired in the red and near-infrared (NIR) spectral regions of the electromagnetic spectrum, where SPM usually dominates the seawater spectral signature[13], [22]. In particular, the wavelength associated to the maximum in remote sensing reflectance increases from green to red up to NIR wavelengths with increasing SPM concentration (SPMC) [13].

According to [13] on the study on Gironde estuary, remote sensing reflectance grows between 400 and 700 nm for moderately high SPM values (35–250 g/m3), while Rrs tends to saturate at these wavelengths for extremely turbid waters (SPMC higher than 250 g/m3) but still considerably increases in the spectral NIR region.

Many satellite radiometers, capable of acquiring information in the visible and NIR spectral
regions, have been exploited so far for such a kind of application. Among them, MODIS is the one operational at a global scale with a good trade-off between spatial and temporal resolution. There are many satellite radiometers capable of acquiring visible and NIR spectral regions such as MODIS with its on-board Earth Observing System (EOS) Terra (since 2000) and Aqua (since 2002) with two spectral bands in the red (band 1, 620–670 nm) and NIR band 2, 841–876 nm) regions at a spatial resolution of 250 m, acquired twice per day, almost all over the world [11]. Several authors have used MODIS single band algorithms as well as the combination of bands for retrieving SPMC in different geographical areas characterized by different SPM features [11], [3].

B. Algorithm

Algorithms for quantification of SPM from water-leaving reflectance fall roughly into one of three families: single band, band ratio or multispectral [25]. These algorithms are described in the following sub-sections.

a) Single Band Algorithms

For low and moderate reflectances, it is easy to detect SPM as there is a linear relationship between SPM and reflectance at any given wavelength (Althuis and Shimwell, 1995). At higher reflectances this relationship becomes non-linear and the reflectance is usually considered to approach asymptotically a maximal "saturation" value [13] where an increase in SPM concentration no longer affects reflectance [2]. Many algorithms have been developed to estimate SPM from reflectance at a single wavelength involving a linear, low reflectance, regime and a monotonic but non-linear high reflectance regime, although various functional forms have been suggested for the latter including logarithmic [3].

The performance of such single band algorithms is generally best for low to moderate reflectances as optimal wavelength will depend on concentration and fixed wavelength algorithms will typically be limited to a certain range of concentrations [6]. Their accuracy depends on the validity of the underlying assumptions, particularly that total backscatter is proportional to SPM concentration and that space-time variability of non-particulate absorption can be neglected as the use of red or near infrared bands is preferred so that non-particulate absorption arises essentially from pure water absorption ([4]. Alternatively, if sufficient wavelengths of data are available, an adaptive algorithm could be envisaged using the basic one-band algorithm but with the retrieval wavelength being chosen differently for each input reflectance spectrum [5],[6].

An interesting variant on these algorithms is the use of algorithms based on the difference between two bands, generally red and near infrared (Ruddick et. al., 2008). These algorithms have similar properties to the single band algorithms but combine the SPM retrieval with a full aerosol correction (Stumpf and Pennock, 1989 as cited in Ruddick et. al., 2008) or a residual correction for aerosols after atmospheric correction [23].

The appropriateness of single band algorithms for SPM estimation means that SPM mapping can be made not just with dedicated ocean color sensors such as MODIS or MERIS but also with a very wide range of optical remote sensors, including SPOT, LANDSAT, ASTER, AVHRR, SEVIRI, etc. [17], [24].

b) Band Ratio Algorithms

Another alternative to single band algorithms is two-band ratio algorithms for SPM estimation [13]. One band algorithms are highly sensitive to backscatter and hence are subject to uncertainties if the mass-specific backscatter coefficient has high natural variability (Ruddick et. al., 2008). In contrast, band ratio algorithms can be designed to be less sensitive to this natural variability since spectrally flat backscatter effects largely cancel when a ratio is taken (Ruddick et. al., 2008) and it is less sensitive to illumination conditions [12]. Band ratio algorithms may however be sensitive to the natural variability of sediment absorption properties since the use of a reflectance ratio shifts the relevant physics from backscattering properties to absorption properties (Moore et al., 1999 cited in Ruddick et. al., 2008).

c) Multispectral Algorithms

With availability of more dedicated ocean color sensors, many more bands of data are available that could improve algorithm performance, if the information is reliable (Ruddick et. al., 2008). The mathematical methods used in multispectral algorithms are quite diverse (Ruddick et. al., 2008). However, this family of algorithms is generally based on a forward model defining reflectance as function of inherent optical properties, including particulate backscatter and absorption, and an inversion procedure to find the model reflectance spectrum that best fits the measured reflectance (Doerffer and Fischer, 1994 cited in Ruddick et. al., 2008). The IOP set corresponding to this best-fitting model reflectance spectrum is then related to SPM concentration.

One operational example of a multispectral SPM algorithm is the standard case 2 water algorithm for MERIS, which uses a forward model based on radiative transfer simulations and a neural network inversion procedure (Doerffer and Schiller, 1997 cited in Ruddick et. al., 2008).

One major advantage of the multispectral algorithms is the opportunity of automatically adapting to a varying mixture of algal and non-algal particles and thus offering greater generality (Ruddick et. al., 2008). In other words, the analysis of multispectral data can provide an estimate of phytoplankton absorption and hence of the contribution of algal particles to total particulate backscatter (Ruddick et. al., 2008). It is no longer necessary to assume, as in the one-band approach, constant SPM-specific particulate backscatter. Moreover, the consistency between the measured reflectance spectrum and the best-fit modelled can provide indications on the quality of the water-leaving reflectance data and on the uncertainty of the retrieved SPM (Ruddick et. al., 2008). However, Ruddick et. al. (2008) points out that such algorithms are still subject to uncertainties relating to conversion from optical properties to mass concentration.

d) Towards Global Algorithms

Even though, the proposed algorithms perform well for the specific region where they were calibrated, they lack consistent accuracy over different geographic regions[16]. Some efforts have been made in the past years to develop a more general algorithm valid for a wide range of geographical and geophysical settings as well as SPM concentrations [11][18]. Nechad et. al proposed a semi-analytical single band algorithm for SPMC retrieving, for different sensors and wavelengths, calibrated using in situ data (SPM range: from ~1 to ~110 g/m^3) from the Southern North Sea, finding an error of about 30% and 40% in calibration and validation respectively [22]. More recently, Han tested different algorithms for retrieving SPMC on a wide range of concentrations (from 0.15 to 2626 g/m^3) and for various coastal environments dominated by river discharge, resuspension or phytoplankton bloom in Europe, French Guiana, North Canada, Vietnam, and China. Among the algorithms tested, the one proposed by Nechad et. Al resulted the best, assuming that the model parameters were adapted using the in situ measurements [22].

These preliminary studies confirmed the uncertainties of such algorithms if applied to different SPMC ranges or geophysical characteristics, suggesting the need of further analyses for a better accuracy assessment [11]. Another source of

uncertainty for these algorithms concerns the implemented atmospheric correction procedures [11], Ruddick et. al., 2008). Even if several atmospheric correction algorithms have been proposed for turbid coastal waters, their performance changes on the basis of the analyzed location and range of SPMC [11]. Moreover, the SPMC values and variations are usually unknown for those areas where no previous studies are done that makes it difficult to understand the significance of an absolute SPMC value [11]. The same difficulty, considering the SPM variability in the spatiotemporal domain, can occur also in the same study area [11]. To explain this variation in the same study [11] gave the example - a SPMC of 50 g/m^3 in an area normally characterized by high SPMC values (e.g., estuarine or coastal area under the influence of very turbid rivers, etc.) could have a low specific impact on the local environment. Instead, the same SPMC value, if registered in areas normally characterized by lower SPM concentrations, might have stronger effects and lead to serious environmental risks [11].

C. Validation
The primary approach to SPM product validation is by comparing the data value for a satellite pixel with an in situ measurement from a location within that pixel and acquired almost simultaneously (in coastal waters, within 1 hour according to the recommendations of the MERIS Validation Team) (Ruddick et. al., [9]. An example of such a comparison is shown in Fig. 1. Differences between in situ and satellite measurements are typically many tens of per cent. Analysis of these differences is a challenging scientific exercise because of the large number of sources of uncertainty both on the satellite-side (SPM algorithm including variability of mass-specific properties, water-leaving reflectance input including atmospheric correction uncertainties, etc.) and on the measurement side (space-time mismatch with satellite pixel, mixing of sample, rinsing/weighing of filters, etc.) [8]. The lack of simultaneous in situ data is a serious shortcoming [7], [1].
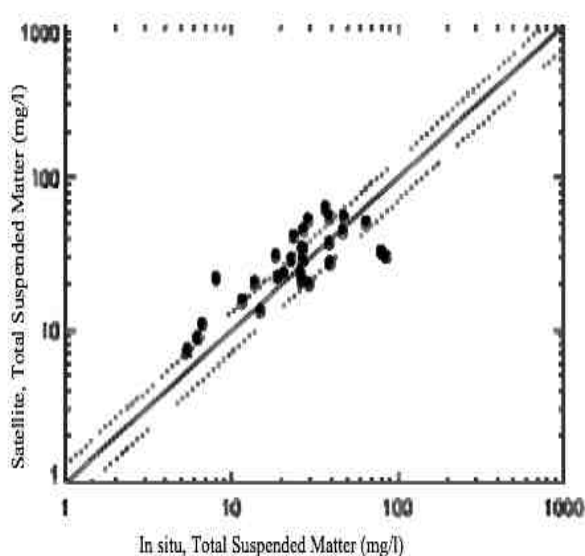

Fig. 1. Validation of TSM derived from the MODIS 678nm band using algorithm (1) against simultaneous in situ measurements in Southern North Sea waters. [Points generally lie within 30% of the 1-1 line for a range of concentrations from 5 to 100 mg/l], Ruddick

SPM algorithm validation using spectroradiometers is also important and removes at least some sources of difference (atmospheric correction) and improves the space-time match of the two datasets [15], [21].

Depending on the needs, it may be more relevant to validate at the level of multitemporal products such as monthly or climatological averages (Ruddick et. al., 2008). Such an approach enables much more in situ data to be used. It can be challenging to understand and trace the causes of satellite/in situ measurement differences because of the asynchronicity of data, even though it is appropriate for establishing the fitness for purpose of such multitemporal products [14]

Although not generally considered as validation, in situ measurements of mass-specific inherent optical properties and study of their natural variability (Astoreca et al., 2006; Babin et al., 2003a; Babin et al., 2003b cited in Ruddick et. al., 2008), provides important information on related product uncertainty (Ruddick et. al., 2008).

D. Quality Control
In addition to a posteriori validation analysis, methods are developimmg for automatic quality control of satellite data products (Ruddick et. al., 2008). Processing flags indicating warning conditions relating to atmospheric correction such as negative water-leaving reflectances or out-of-bound aerosol products are a standard feature of a functional ocean color processing chains (Robinson et al., 2003 cited in Ruddick et. al., 2008). Multispectral inversion algorithms also allow (partial) assessment of product uncertainty by calculating the range of SPM values that could correspond to a reasonable spectral fit between the satellite measurement and the modelled reflectance that would result from the SPM algorithm output (Ruddick et. al., 2008). This product uncertainty can be output in map form along with the product itself as similar to those generated for chlorophyll products (Peters et al., 2005 cited in Ruddick et. al., 2008).

II. MATERIALS AND METHODS

A. Study Site
Mamloo Dam, is a dam in the Central Alborz mountain range of northern Iran near to the Mount Damavand. It is located 35 kilometres west of Tehran and 49 kilometres southwest of Mount Damavand.

B. Field Data
Field data was collected from the dam on 8/28/2015 and 8/27/2016 for all the 12 sampling sites (Fig. 2). Systematic sampling is used to select the sites. The following data was collected.
- Water sample
- Radiometer reflectance measurements
- Backscattering and florescence measurement
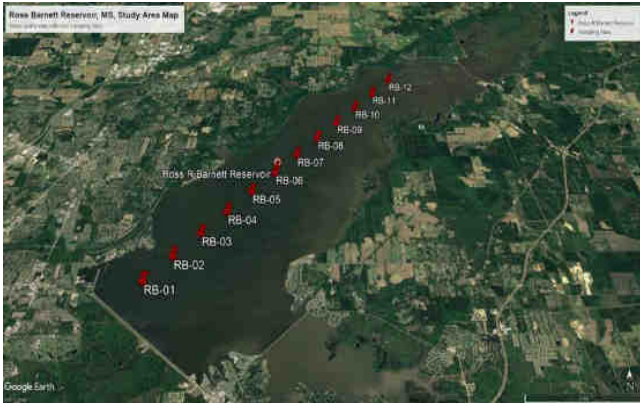- Secchi depth measurement
- dam Depth

Fig. 2. Google Earth Imagery of Mamloo Dam and the sample sites

C. Data Processing and Lab Procedures

The collected samples are filtered and processed to obtain the following:

- SPM absorption
- SPM concentration
- SPM backscattering
- Chlorophyll a absorption
- Phycocyanin absorption
- Spectrophotometer measurement of absorption

D. Algorithm Development

The algorithm is developed using semi-analytical approach. Out of the 12 sampling sites, 8 were used for algorithm development and the 4 sites were used for validation. The validation sites were identified by simple random sampling. To develop SPM algorithm focusing on NAP, the Rrs is computed and subtracted systematically from the combination of components containing the absorption of water, chl a, NAP, and CDOM and backscattering by water, Chl a, and SPM using the following equation [10].

$$Rrs = 0.54(f/Q)(bb/(a+bb)) \qquad (1)$$

Where 0.54 accounts for the Fresnel reflectivity at the sea surface. The proportionality constant (f/Q) values of 0.0922 was used. To obtain the Rrs of NAP, first Rrs without NAP was calculated. Then, this Rrs without NAP is subtracted from the total Rrs from MODIS to obtain the NAP Rrs. The satellite Rrs from MOODISMODIS is atmospherically corrected. To come up with the correct wavelength, single band and band ratio methods were used. Using R2, Root Mean Squared Error (RMSE) and liner and polynomial Regression , among the tested, the best algorithm is selected.

III. RESUTS

The NAP values were obtained by reducing Chl-a form SPM. Then NAP is used to get the algorithm. Some calculations were done to find the best algorithm such as single band linear relationship and ratio of the bands.

A) Single Band Linear Relationship

The slop of bands of MODIS in visible wavelengths 412, 443, 488, 531, 547, and 667 nm were compared. Then, the slop of all of them is observed by comparing it to the slop of NAP and identified Rrs 547 as a suitable wavelength for direct linear relationship. Then, additional coefficients were added to come up with the following algorithm:

NAP = Rrs 547 * 303 – 3.38   (2)

Rrs at 547nm is multiplied by 100 to adjust close to 0 values to have over 1. However, the R2 was very low at 0.43. The fig. 3vshows the low relationship.
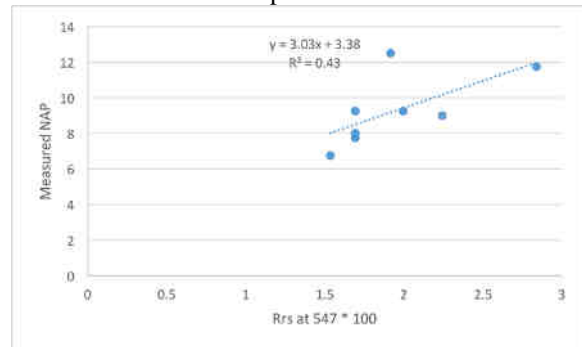

Fig. 3. Single-band linear Rrs at 547nm

B) Band Ratio

We compared the slop of bands of MODIS in visible wavelengths 412, 443, 488, 531, 547, and 667 nm. After testing all other ratios of bands, we found out that the ratio of 547/531 yielded a higher R2 value of 0.53 as shown in the Fig. 4.
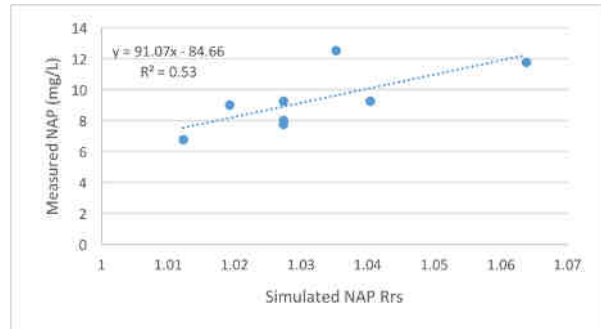

Fig. 4. A linear regression for measured NAP and band ratio of total Rrs at 547nm and 531nm

To improve the reliability of the algorithm and the R2 value, simulated Rrs from backscattering and absorption is calculated using equation (1). To get Rrs(λ)(NAP) and come up with semi-analytical algorithm, the following procedures were followed:

➢ **Obtain bb of water without SPM**

➢ bb of water is obtained from Smith and Baker (1981)
Then the bb of water is used without adding bb of SPM as most of the backscattering comes from NAP. As the objective is to obtain Rrs without NAP
Obtain absorption without SPM
Then absorption of water is obtained from Mueller et. al. (2003)

1. The absorption of CDOM is calculated by extrapolating using slop and absorption of CDOM at 440nm (calculated using the average between 434nm – 446nm absorption values).
2. Thus, absorption (NAP=0) is obtained by summing absorption of water, and CDOM, Chl-a and Phycocyanin.

➢ Obtaining Rrs(NAP)
1. By using Equation 1: (Rrs(λ) = 0.54 (f/Q) * bb/(a+bb)) , Rrs(λ)(NAP=0) is calculated.

2. Finally, by subtracting Rrs(λ)(NAP=0) from Satellite Rrs, Rrs(λ)(NAP) is obtained for both Rrs 531nm and 547nm.

➤ Apply band ratio method
1. RrsNAP at 547nm is divided by RrsNAP at 531nm to get the ratio
2. Compare it with measured NAP in scatter plot
3. Obtained R2 value of 0.52 with linear regression that is slightly less than R2 obtained using total Rrs as shown in Fig. 4. With polynomial regression 0.54 R2 is obtained as shown in the Fig. 5.
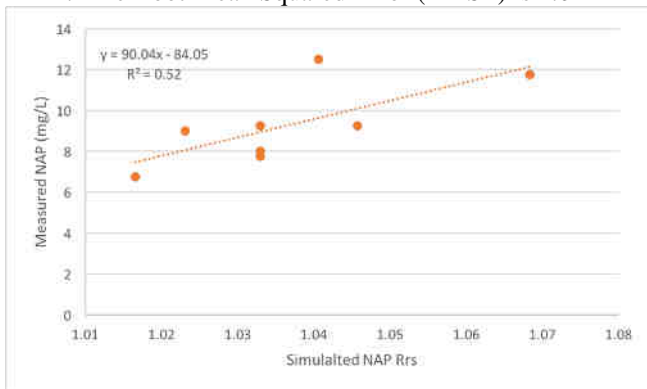4. The Root Mean Squared Error (RMSE) is 1.04

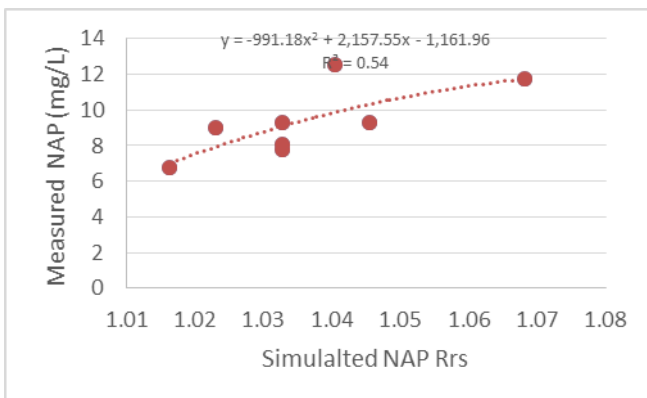Fig. 5. A linear regression for measured NAP and band ratio of total Rrs(NAP) at 547nm and 531nm

Fig. 6. A polynomial regression for measured NAP and band ratio of total Rrs(NAP) at 547nm and 531nm

Thus, NAP concentration can be obtained by getting Rrs of NAP using the above steps and by calculating using the following equation:

$$NAP = 90.04 * \frac{R_{rs(NAP)}547}{R_{rs(NAP)}531} - 84.05 \quad (3)$$

$$NAP = -991.18 * \left(\frac{R_{rs(NAP)}s547}{R_{rs(NAP)}531}\right)^2 + 2,157.55 * \left(\frac{R_{rs(NAP)}s547}{R_{rs(NAP)}531}\right) - 1,161.96 \quad (4)$$

C) Rrs using Absorbance

In the above single band and band ratio procedures, absorption coefficient is used that is calculated using specific absorption coefficient at each wavelength. In this case however, only the absorption is used to get the Rrs without NAP. An identical R2 of 0.52 and RMSE of 1.04 is found.
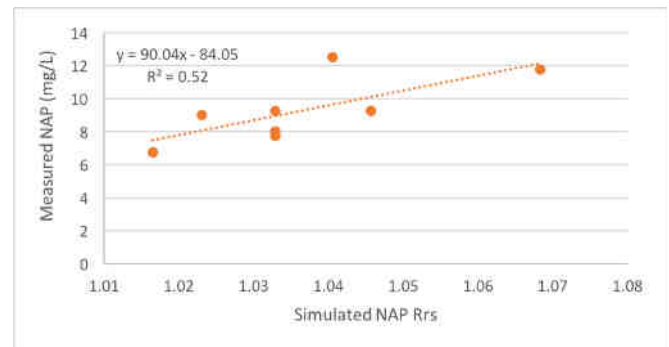

Fig. 7. A linear curve for measured NAP and band ratio of Rrs(NAP) at 547nm and 531nm calculated using Absorbance.

Thus, NAP concentration can be obtained by getting Rrs of NAP using the above steps and by calculating using the following equation:

$$NAP = 90.04 * \frac{R_{rs(NAP)}547}{R_{rs(NAP)}531} - 84.05 \quad (5)$$

D) Validation

The final algorithms (equation 4 and 5) were validated using four sampling sites. The measured and the estimated NAP concentration is compared. The result of equation 4 was very good with the R2 value of 0.93. The RMSE was also very good at 0.72. The Fig. 8 shows the relationship between the measured and estimated NAP concentration.
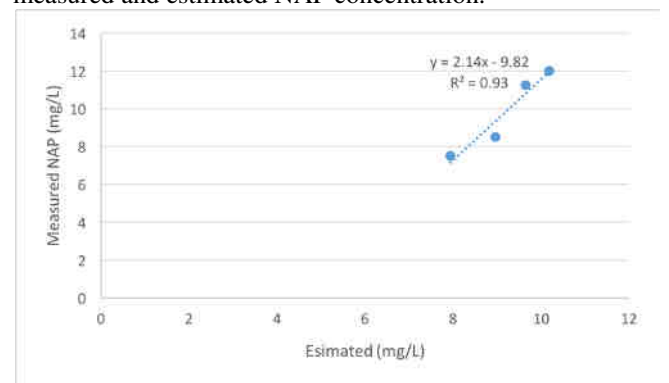

Fig. 8. Linear regression for measured NAP and estimated NAP using equation 4

While testing the polynomial equation (4), a less accurate R2 value of 0.90 is obtained. However, the RMSE (0.63) is better than the value obtained from equation 3 (Fig. 9). Consequently, equation 4 is the best equation because of its lower RMSE.
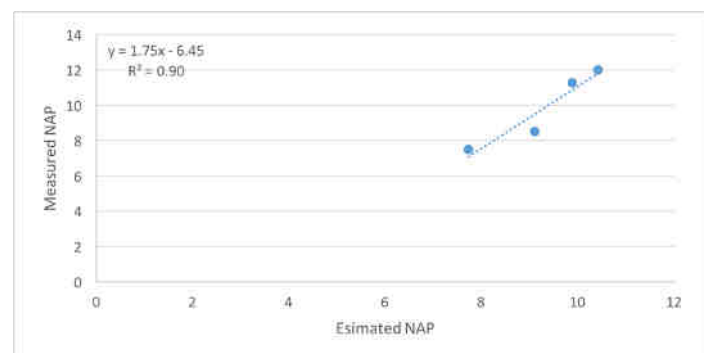

Fig. 9. Linear regression for measured NAP and estimated NAP using equation 5.

IV. DISCUSSION

a. Usefulness of Algorithms Developed from Satellite Data

Satellite remote sensing saves both time and money as compared to airborne remote sensing as the data is freely available such as MODIS. MODIS a dedicated ocean color satellite (Ruddick et. al., 2008), even though it is also used for other purposes. MODIS is operational at a global scale with a good trade-off between spatial and temporal resolution. There are many satellite radiometers capable of acquiring visible and NIR spectral regions such as MODIS with its on-board Earth Observing System (EOS) Terra (since 2000) and Aqua (since 2002) with two spectral bands in the red (band 1, 620–670 nm) and NIR band 2, 841–876 nm) regions at a spatial resolution of 250 m, acquired twice per day, almost all over the world [11]. Several authors have used MODIS single band algorithms as well as the combination of bands for retrieving SPMC in different geographical areas characterized by different SPM features [11]. The use of MODIS will make it easy to create future data using the developed algorithm and procedure.

b. Assessment of the Developed Algorithms

Considering that Mamloo Dam is shallow and susceptible to particulate re-suspension due to human activity and the Pearl River is expected to have high SPMC. This reduces the performance of single band and band ratio algorithms as pointed out by Ruddick et. al. (2008). Even though, it is suggested to alternatively use near infrared bands for high concentrations, the atmospheric correction is not applied in the MODIS satellite data used for the algorithm development. Thus, our test of single band algorithm was concentrated in the visible region. The Multispectral algorithms are not used in this study due to time constraints.

Consequently, the focus was given to band-ratio algorithm development that performs well in both low and high concentration [13], after subtracting optically active constituents, that are not relevant in this case. However, we could not test the ratio between visible around 550 nm with near infrared bands as the near infra-red bands were not readily available in our project. When tested, band ratio algorithms gave a better result compared with single band algorithm. The band ratio of 547 to 531 was selected as it gave better result as compared to all other band ratios.

CONCLUSION

To sum up, SPM specifically NAP poses a serious threat to the quality of the Mamloo Dam. This is because NAPs contain pollutants and clay particles that can cause serious health problems to the aquatic life. Algal particulates also can cause a serious danger but their difference in nature and impact as compared to NAP, laid the foundation for focusing on NAP.

Band-ratio algorithm, after removing the influences of other IOPs, gave a good result. Better result could have been obtained if band ratio between visible region (around 550nm) and near infrared region was used. The ratio between Rrs (NAP) at 547nm and Rrs (NAP) at 531nm gave a good result with strong correlation (up to $R^2=0.93$) when validating the result.

Procedurally, Rrs calculated using absorbance values directly coming from spectrophotometer gave almost identical result when compared with Rrs values calculate using absorption that is obtained using specific absorption coefficients. This finding reduces the time to develop algorithms.

The R2 value obtained using a linear regression between total Rrs and measured NAP (0.53) is slightly higher than the R2 value between simulated NAP Rrs and measured NAP (0.52). However, relaying on the total Rrs will not guarantee good correlation in different seasons and locations. Most importantly, comparing NAP Rrs and measured NAP, two equations are tested, linear and polynomial. The polynomial equation (4) showed a better R2 of 0.54 as compared 0.52 R2 for the linear equation (3). However, to choose the best algorithm, the RMSE is important. The measured NAP correlated with estimated NAP, both gave a high R2 of 0.93 and 0.90 for equation 3 (linear) and 4 (polynomial) respectively. However, when looking at the RMSE there is a noticeable difference in favor of equation 4 (polynomial) that makes it the best equation. The RMSE for equation 4 is as low as 0.63 as compared with 0.72 for equation 3 (linear).

REFERENCES

1. A Sescu, L Taoudi, M Afsar , Iterative control of Görtler vortices via local wall deformations, Theoretical and Computational Fluid Dynamics 32 (1), 63-72
2. A Sescu, L Taoudi, MZ Afsar, DS Thompson Control of Gortler vortices by means of staggered surface streaks, 46th AIAA Fluid Dynamics Conference, 3950
3. Barzin, Razieh, Amin Shirvani, and Hossein Lotfi. "Estimation of daily average downward shortwave radiation from MODIS data using principal components regression method: Fars province case study." International agrophysics 31, no. 1 (2017): 23-34.
4. Bastani, A. F., & Damircheli, D. (2017). An adaptive algorithm for solving stochastic multi-point boundary value problems. Numerical Algorithms, 74(4), 1119-1143.
5. Bastani, A. F., Ahmadi, Z., & Damircheli, D. (2013). A radial basis collocation method for pricing American options under regime-switching jump-diffusion models. Applied Numerical Mathematics, 65, 79-90.
6. Capper, N., 2006. The Effects of suspended sediment on the aquatic organisms Daphnia magna and Pimephales promelas.
7. Damircheli, D., & Bhatia, M. (2019). Solution Approaches and Sensitivity Analysis of Variational Inequalities. In AIAA Scitech 2019 Forum (p. 0977).
8. DAMIRCHELI, ROYA, HAMID MIRZADEH, HERISH MORADI, YASSER GHAZIZADEH, and ZOHREH JALALI. "ELECTROSPUN NANOFIBROUS SCAFFOLDS BASED ON ALGINATE FOR SKIN TISSUE ENGINEERING." (2014).
9. DAMIRCHELI, ROYA, HAMID MIRZADEH, HERISH MORADI, YASSER GHAZIZADEH, and ZOHREH JALALI. "ELECTROSPUN NANOFIBROUS SCAFFOLDS BASED ON CHITOSAN FOR SKIN TISSUE ENGINEERING." (2014).
10. Dash, P., Walker, N.D., Mishra, D.R., Hu, C., Pinckney, J.L. and D'Sa, E.J., 2011. Estimation of cyanobacterial pigments in a freshwater lake using OCM satellite data. Remote Sensing of Environment, 115(12), pp.3409-3423.
11. Di Polito, C., Ciancia, E., Coviello, I., Doxaran, D., Lacava, T., Pergola, N., Satriano, V. and Tramutoli, V., 2016. On the potential of robust satellite techniques approach for SPM monitoring in coastal waters: implementation and

APplication Over the Basilicata Ionian Coastal Waters Using MODIS-Aqua. Remote Sensing, 8(11), p.922.

12. Doxaran, D., Froidefond, J.M. and Castaing, P., 2003. Remote-sensing reflectance of turbid sediment-dominated waters. Reduction of sediment type variations and changing illumination conditions effects by use of reflectance ratios. Applied Optics, 42(15), pp.2623-2634.

13. Doxaran, D., Froidefond, J.M., Lavender, S. and Castaing, P., 2002. Spectral signature of highly turbid waters: Application with SPOT data to quantify suspended particulate matter concentrations. Remote sensing of Environment, 81(1), pp.149-161.

14. Ghanbari, Gh, and Mohammad HadiFarahi. "Optimal control of a delayed HIV infection model via Fourier series." Journal of Nonlinear Dynamics 2014 (2014).

15. Ghanbari, Gh, and Mohammad HadiFarahi. "Optimal control strategy for a HIV infection model via Fourier series." Journal of Applied Mathematics, Statistics and Informatics (JAMSI) 9, no. 2 (2013).

16. Han, B., Loisel, H., Vantrepotte, V., Mériaux, X., Bryère, P., Ouillon, S., Dessailly, D., Xing, Q. and Zhu, J., 2016. Development of a semi-analytical algorithm for the retrieval of suspended particulate matter from remote sensing over clear to very turbid waters. Remote Sensing, 8(3), p.211.

17. JALALI, ZOHREH, ASL VAHID HADDADI, Iman Shabani, MasoudSoleimani, Abbas Shafiee, and Roya Damircheli. "Improving biocompatibility of the polyacrylonitlienanofibrous scaffolds." (2014).

18. JALALI, ZOHREH, ASL VAHID HADDADI, Iman Shabani, MasoudSoleimani, and Roya Damircheli. "A novel method for producing gelatin nanofibers contains hydroxyapatite nanoparticles." (2014).

19. John R. Jensen. 2014. Remote Sensing of the Environment: An Earth Resource Perspective. Pearson Education Limited: Edinburgh

20. Kjelland, M.E., Woodley, C.M., Swannack, T.M. and Smith, D.L., 2015. A review of the potential effects of suspended sediment on fishes: potential dredging-related physiological, behavioral, and transgenerational implications. Environment Systems and Decisions, 35(3), pp.334-350.

21. M Bhatia, L Taoudi Assessment of Stabilized Sensitivity Analysis Approach For High-Dimensional Chaotic Systems, AIAA Scitech 2019 Forum, 0170

22. Nechad, B., Ruddick, K.G. and Park, Y., 2010. Calibration and validation of a generic multisensor algorithm for mapping of total suspended matter in turbid waters. Remote Sensing of Environment, 114(4), pp.854-866.

23. Ourang, Armin, SoheilPilehvar, MehrzadMortezaei, and Roya Damircheli. "Effect of aluminum doped iron oxide nanoparticles on magnetic properties of the polyacrylonitrile nanofibers." Journal of Polymer Engineering 37, no. 2 (2017): 135-141.

24. Pathak, Rohit, Razieh Barzin, and Ganesh C. Bora. "Data-driven precision agricultural applications using field sensors and Unmanned Aerial Vehicle." International Journal of Precision Agricultural Aviation 1, no. 1 (2018).

25. Ruddick, K., Nechad, B., Neukermans, G., Park, Y., Doxaran, D., Sirjacobs, D. and Beckers, J.M., 2008. Remote sensing of suspended particulate matter in turbid waters: state of the art and future perspectives. Ocean Optics XIX, pp.6-10.